Catalysis Today 181 (2012) 138–147

Contents lists available at ScienceDirect

Catalysis Today

journal homepage: www.elsevier.com/locate/cattod

Mechanistic aspects of the selective methanation of CO over Ru/TiO_2 catalyst

Paraskevi Panagiotopoulou, Dimitris I. Kondarides, Xenophon E. Verykios*

Department of Chemical Engineering, University of Patras, GR-26504 Patras, Greece

ARTICLE INFO

Article history:
Received 2 March 2011
Received in revised form 11 May 2011
Accepted 27 May 2011
Available online 28 June 2011

Keywords:
Ruthenium
TiO_2
Selective methanation
Carbon monoxide
Carbon dioxide
Hydrogen
FTIR
Transient-MS

ABSTRACT

The mechanism of selective methanation of CO/CO_2 over $5\%Ru/TiO_2$ catalyst is investigated employing *in situ* FTIR spectroscopy (DRIFTS) and transient mass spectrometry techniques. It is shown that interaction of the prereduced catalyst with the reaction mixtures results in the development of various Ru-bonded carbonyl species on reduced and partially oxidized sites as well as on sites located at the metal-support interface. The nature and population of these species depend strongly on feed composition and reaction temperature. Results of the present study confirm our previous suggestion that the mechanism of CO methanation includes both dissociative and associative reaction pathways. The former, which dominates at lower reaction temperatures, involves hydrogenation of surface carbon produced by dissociative adsorption of CO, whereas the latter involves hydrogenation of CO species adsorbed at the metal-support interface. At low temperatures, typically <250 °C, dissociation of CO results in accumulation of adsorbed oxygen species which cannot be removed from the catalyst surface, rendering it inactive. Catalytic activity is restored at higher temperatures, where partially oxidized sites are reduced efficiently by adsorbed hydrogen atoms. The associative reaction pathway is the only one which is operable under conditions of CO_2 methanation and proceeds via intermediate formation of carbonyl species at the metal-support interface, produced by the RWGS reaction. Selective methanation of CO in CO/CO_2 mixtures occurs efficiently under conditions where the dissociative reaction pathway is operable and the associative reaction pathway is completely suppressed.

1. Introduction

Interest in the CO methanation reaction has grown significantly during the last few years as a result of recent advancements in fuel cell technology and the need for development of fuel processors capable of converting carbonaceous fuels into hydrogen [1–4]. In such systems, the CO methanation reaction Eq. (1) can be used as the final purification step of reformate gas to reduce CO concentration to the extremely low levels (<50 ppm) dictated by the poisoning limit of PEM fuel cell electrodes [5].

$$CO + 3H_2 \leftrightarrow CH_4 + H_2O, \quad \Delta H^\circ = -206\,kJ\,mol^{-1} \tag{1}$$

However, depending on operating conditions and catalyst employed, reaction (1) may occur in parallel with the undesired methanation of CO_2 Eq. (2), which consumes significant quantities of hydrogen, as well as with the reverse water–gas shift (RWGS) reaction Eq. (3), which shifts CO_2 to CO [1,2].

$$CO_2 + 4H_2 \leftrightarrow CH_4 + 2H_2O, \quad \Delta H^\circ = -165\,kJ\,mol^{-1} \tag{2}$$

$$CO_2 + H_2 \leftrightarrow CO + H_2O, \quad \Delta H^\circ = 41.1\,kJ\,mol^{-1} \tag{3}$$

As a result, efforts are focused toward the development of selective CO methanation catalysts, with sufficiently high activity at low temperatures, able to suppress both CO_2 methanation and RWGS reactions. Supported ruthenium and rhodium catalysts seem to be able to meet the above criteria and, therefore, have been widely investigated [1–3,6,7].

Although the mechanism of both CO [8–15] and CO_2 [16–24] hydrogenation reactions has been extensively studied, it is not clear, so far, which of the adsorbed species detected on the catalyst surface are active and define catalytic activity for each reaction. In our recent work [1] a detailed investigation of the methanation of CO, CO_2 and their mixtures has been carried out over $5\%Ru/TiO_2$ catalyst, which has been shown to exhibit high activity, selectivity and long-term stability for the selective methanation of CO under realistic reaction conditions. Evidence has been provided that methanation of CO occurs via two distinct reaction pathways; The first one, which dominates at lower reaction temperatures, involves hydrogenation of surface carbon produced by dissociative adsorption of CO, whereas the second involves direct hydrogenation of adsorbed CO species [25]. The latter pathway has been proposed to be the only one that is operable under conditions of CO_2 methanation and proceeds via intermediate formation of Ru-bonded carbonyls by the RWGS reaction at the metal-support interface.

* Corresponding author. Tel.: +30 2610 991527; fax: +30 2610 991527.
E-mail address: verykios@chemeng.upatras.gr (X.E. Verykios).

0920-5861/$ – see front matter © 2011 Elsevier B.V. All rights reserved.
doi:10.1016/j.cattod.2011.05.030

In the present work, the reaction mechanism over 5%Ru/TiO_2 catalyst is further investigated employing *in situ* FTIR and transient mass spectrometry (transient-MS) techniques. The aim is to identify the nature of active sites, adsorbed species and reaction intermediates involved in the CO/CO_2 methanation reactions and, subsequently, to propose possible mechanistic schemes for both reactions.

2. Experimental

2.1. Catalyst preparation and characterization

The Ru/TiO_2 catalyst was prepared employing the wet impregnation method using TiO_2 (Degussa P25) as support and $Ru(NO)(NO_3)_3$ (Alfa) as ruthenium precursor salt [1]. The nominal Ru loading of the catalyst thus prepared was 5 wt%. The catalyst was characterized with respect to its specific surface area (BET), phase composition and crystallite size of TiO_2, and platinum dispersion, employing physical adsorption of N_2 (77 K), X-ray diffraction (XRD), and selective chemisorption of H_2, respectively. Details on the apparatus and procedures used can be found elsewhere [26].

2.2. In situ FTIR spectroscopy

Fourier transform infrared (FTIR) experiments were carried out using a Nicolet 6700 FTIR spectrometer equipped with a diffuse reflectance (DRIFT) cell (Spectra Tech), an MCT detector and a KBr beam splitter. The exit of the DRIFT cell was connected to a non-dispersive infrared (NDIR) analyzer (Binos) for on-line measurement of CO and CO_2 concentrations. In a typical experiment, the catalyst powder was heated at 450 °C under He flow for 10 min and then reduced in flowing hydrogen (20%H_2 in He) at 300 °C for 60 min. The cell was then flushed with He at 450 °C for 10 min and subsequently cooled to the desired temperature under He flow for 10 min. During the cooling stage, background spectra were collected at temperatures of interest. The flow was then switched to a gas mixture consisting of either 0.5%CO + x%H_2 or 1%CO_2 + x%H_2 (x = 0–12) and spectra were obtained at selected feed composition after equilibration for 15 min-on-stream. After recording the spectrum, the flow was switched to the next selected feed composition. In all experiments, the total flow rate through the DRIFT cell was 30 cm^3 min^{-1}.

2.3. Transient mass spectrometry studies

Transient-MS experiments were carried out using the apparatus and following the procedures which have been described in detail elsewhere [25,27,28]. Briefly, an amount of catalyst (150 mg) was placed in a quartz microreactor and reduced with hydrogen at 300 °C. The sample was then purged with He at 500 °C for 10 min to remove adsorbed species from the catalyst surface and subsequently cooled to the desired temperature under He flow. Transient experiments were then carried out by switching the flow to the desired feed composition (0.5%CO + 5%H_2, 1%CO_2 + 5%H_2 or 0.5%CO + 1%CO_2 + 5%H_2 in He) with the use of a chromatographic valve equipped with an electronic actuator. The feed also contained a small amount of an inert gas (0.5%Ar), the response curve of which represents the flow pattern and the residence time distribution of gaseous reactants flowing through the reactor and the transportation lines. In all experiments, the total flow rate through the reactor was 30 cm^3 min^{-1}. An Omnistar/Pfeiffer Vacuum mass spectrometer (MS) was used for on-line monitoring of effluent gas composition, following the procedures described in detail elsewhere [25].

3. Results and discussion

3.1. Catalyst characterization

Results of catalysts characterization showed that the specific surface area (BET) of the 5%Ru/TiO_2 catalyst was 42 m^2 g^{-1}, the Ru dispersion was 21% and its mean crystallite size (d_{Ru}) was 4.5 nm. The titanium dioxide support was found to consist of 75% anatase with a primary crystallite size (d_{TiO_2}) of 25 nm [26].

3.2. Effects of H_2 concentration on CO/CO_2 methanation reactions studied by DRIFTS

3.2.1. Methanation of CO

DRIFT spectra obtained over the Ru/TiO_2 catalyst, following exposure to 0.5%CO (in He) at 200 °C for 15 min (trace a) and subsequent addition of x%H_2 (x = 0–12) in the mixture (traces b–i), are shown in Fig. 1A. The spectrum recorded in the absence of H_2 (trace a) is characterized by bands in the ν(CO) region attributed to carbonyl species adsorbed on ruthenium, and by bands located below 1700 cm^{-1} (not all shown for clarity), which are due to adsorbed species associated with the support. The band located at 2052 cm^{-1} is attributed to linear CO adsorbed on reduced Ru crystallites (Ru_x-CO) [29–34], whereas the bands at 2136 and 2076 cm^{-1} can been assigned to two different types of multicarbonyl species on partially oxidized Ru sites ($Ru^{n+}(CO)_x$) [25,29,30]. Formation of the latter species is known to take place via oxidative disruption of small Ru clusters with the participation of hydroxyl groups of the support [33,35]. The broad spectral feature observed as a low-frequency (LF) shoulder of the 2052 cm^{-1} band may contain contributions from several species, including linear CO on small and less perfect Ru crystallites [35], isolated Ru^0-CO diluted in an oxidized environment [36], monocarbonyls adsorbed on partially oxidized Ru [13,29,30], and CO adsorbed at the metal-support interface [25,29]. Results of our previous study [25] indicated that the LF shoulder contains a contribution from Ru^{n+}-CO species, i.e., CO adsorbed in the vicinity of Ru–O sites created via dissociative adsorption of CO on reduced ruthenium crystallites:

$$CO + Ru_x \leftrightarrow Ru_x\text{-}CO \quad (4)$$

$$Ru_x\text{-}CO + Ru_x \leftrightarrow Ru_x\text{-}C + Ru\text{-}O \quad (5)$$

Regarding the low-frequency (LF) "tail" of the carbonyl bands, which extends down to 1900 cm^{-1}, it may contain a contribution from (TiO_2)Ru-CO species, i.e., CO adsorbed on Ru sites located at the metal-support interface [25]. Bands due to such species have been reported for a number of noble metals dispersed on reducible supports, including Pt/TiO_2 [27,37], $RuTiO_2(Ca^{2+})$ [29], Au/TiO_2 [38], Pt/CeO_2 [39,40] and Pd/CeO_2 [41], as well as Pt/TiO_2 catalysts doped with alkali [28] or alkaline earth [42] metals. The low frequency of these bands has been attributed to the strong electron-donating properties of noble metal (NM) atoms located at the metal-support interface (e.g., NM-Ti^{3+} sites), which originate from strong interaction with the reducible support [27,28,40,42,43]. It may be noted that the high CO-methanation activity of Rh/TiO_2 catalyst, compared to Rh/MgO or SiO_2, has been attributed to electronic interactions between the TiO_2 and the dispersed metal [44].

Addition of 0.45%H_2 in the reaction mixture does not affect appreciably the intensity or location of bands at 2136 and 2076 cm^{-1} attributed to $Ru^{n+}(CO)_x$ species (trace b). In contrast, it results in a small decrease of the relative intensity of the Ru_x-CO band at 2052 cm^{-1}, which is accompanied by a broadening and red shift of LF bands located at 2050–1900 cm^{-1}. The observation that the integral intensity of carbonyl bands does not change appreciably indicates that, at temperature of 200 °C, the presence of hydrogen does not influence to a large extent the surface coverage

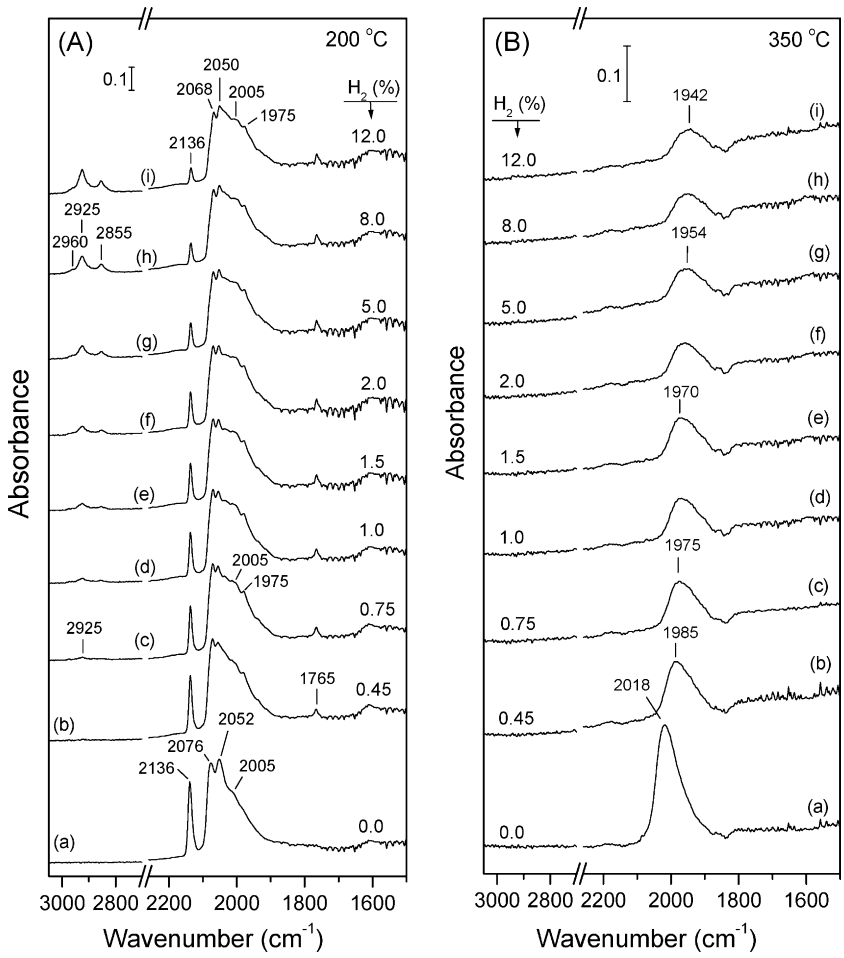

Fig. 1. DRIFT spectra obtained at (A) 200 °C and (B) 350 °C following interaction of Ru/TiO_2 catalyst with 0.5% CO (in He) for 15 min (traces a) and subsequent exposure to 0.5%CO + x%H_2 (x = 0.45–12%) mixtures (traces b–i).

of CO. However, the red shift of carbonyl bands indicates weakening of the C–O bond strength, which may be attributed to the presence of adsorbed species like hydrogen and/or carbon in the vicinity of Ru adsorption sites [13,32,44,45]. It is well known that hydrogen [45] and carbon [32] atoms bonded to the metal surface may induce such an effect by increasing the availability of electrons for back-bonding from the metal to the adsorbed CO molecules [45]. The presence of hydrogen in the feed may also result in reduction of the TiO_2 surface in the vicinity of the metal crystallites [27]. Thus, the observed increase of the intensity of LF bands may be, at least in part, due to creation of additional sites with enhanced electron-donating properties at the metal-support interface (e.g., Ru-Ti^{3+} sites) and, therefore, increased population of (TiO_2)Ru-CO species [27,28,42]. Admission of hydrogen in the feed also results in the development of a weak band located at 1765 cm^{-1}, the intensity of which does not change appreciably with increase of H_2 concentration (traces b–i). Bands in this region have been previously observed under similar reaction conditions over Ru/TiO_2 [30], Ru/Al_2O_3 [30,32] and Ru/SiO_2 [46,47] catalysts and were attributed to bridge-bonded CO on Ru crystallites [30,46,47] or to an μ-bonded carbonyl complex in which both the carbon and oxygen atoms are coordinated with ruthenium surface [32]. The possibility that band at 1765 cm^{-1} is due to another type of surface species cannot be excluded.

Stepwise increase of the concentration of H_2 in the gas stream from 0.45 to 12% results in a progressive decrease of the intensity of the bands located at 2136 and 2076 cm^{-1}, indicating that $Ru^{n+}(CO)_x$ species are not favored in strongly reducing environments. In contrast, bands located below 2050 cm^{-1} are not affected appreciably by the presence of excess H_2 in the feed. It is of interest to note that increasing H_2 concentration results in the progressive development of three bands located at 2960, 2925 and 2855 cm^{-1} (traces c–i), which can be assigned to C–H stretching vibrations in methyl groups ($CH_{3,ad}$) and to symmetric and asymmetric C–H vibrations in methylene groups ($CH_{2,ad}$), respectively [9,13–15]. These species may be formed via successive hydrogenation of carbon atoms produced via dissociative adsorption of CO (see Eqs. (4) and (5)) by adsorbed hydrogen atoms, which may eventually lead to production of methane in the gas phase [9,10,12–15]:

$$C_{(S)} \xrightarrow{H_{(S)}} CH_{(S)} \xrightarrow{H_{(S)}} CH_{2(S)} \xrightarrow{H_{(S)}} CH_{3(S)} \xrightarrow{H_{(S)}} CH_4 \quad (6)$$

However, accumulation of $CH_{x,ad}$ species on the catalyst surface (Fig. 1A) indicates that production of methane is not favored at the temperature of 200 °C, where this set of experiments was conducted. In fact, measurements at the exit of the IR cell with the CO/CO_2 analyzer showed that conversion of CO increased from 0 to 6.5% with increasing H_2 content from 0 to 1.5% (stoichiometric, Eq. (1)), respectively, and did not change, practically, upon further increasing H_2 concentration. It should be noted, however, that these measurements may only provide qualitative information, related, for example, to the onset of the CO/CO_2 methanation and RWGS reactions.

A similar set of experiments was conducted at 350 °C and results obtained are shown in Fig. 1B. It is observed that the spectrum recorded in the absence of H_2 (trace a) consists of a single asymmetric band located at 2018 cm^{-1}, which can be attributed to Ru_x-CO

species. The red shift of the Ru_x-CO band from 2052 cm^{-1} at 200 °C (Fig. 1A, trace a) to 2018 cm^{-1} at 350 °C (Fig. 1B, trace a) is consistent with the decrease of the dipole–dipole coupling with decreasing coverage [37,48]. It is possible that the band centered at 2018 cm^{-1} contains a contribution from (TiO_2)Ru-CO species in its LF tail [25]. Addition of 0.45%H_2 in the gas stream results in a red shift of the 2018 cm^{-1} band by more than 30 cm^{-1} (trace b), which, as discussed above, can be attributed to the presence of electron-donating species in the vicinity of Ru adsorption sites. In addition, the integral intensity of the band decreases by a factor of 2 in the presence of 0.45%H_2, indicating that the population of adsorbed CO species decreases due to competitive adsorption of H_2 and CO on the Ru surface. Under these conditions, conversion of CO measured at the exit of the DRIFT cell was 17%. Further increase of H_2 concentration in the reaction mixture from 0.45% (trace b) to 12% (trace i) results in an additional red shift of the band from 1985 cm^{-1} to 1942 cm^{-1} and a further, but less pronounced, decrease of its intensity. These observations may be explained by considering that, as discussed above, the band contains contributions from both Ru_x-CO and (TiO_2)Ru-CO species. Results of our previous study [25] showed that both species are active for the CO methanation reaction, but hydrogenation of Ru_x-CO is much faster than that of (TiO_2)Ru-CO species in this temperature range. Thus, the relative population of the latter species, which is responsible for the LF tailing part of the band, is expected to increase with increase of H_2 content in the feed, thereby resulting in the observed shift of the band maximum toward lower wavenumbers.

It is of interest to note that, in contrast to what was observed at 200 °C (Fig. 1A), interaction of CO + x%H_2 mixtures with the catalyst surface at 350 °C (Fig. 1B) did not result in the appearance of bands attributable to CO adsorbed on partially oxidized Ru sites (2136 and 2076 cm^{-1}), or $CH_{x,ad}$ species (bands at 2800–3000 cm^{-1}). The absence of bands due to carbonyls adsorbed on Ru^{n+} sites indicates that, at temperature of 350 °C, the population of Ru-O sites is significantly suppressed, probably due to reduction by H_2 and/or CO:

$$\text{Ru-O} + H_2 \rightarrow H_2O + Ru_x \quad (7)$$

$$\text{Ru-O} + CO \rightarrow CO_2 + Ru_x \quad (8)$$

Reaction (7) seems to be the one that dominates under these conditions, because only negligible amounts of CO_2 were measured at the exit of the cell.

Regarding the absence of bands due to $CH_{x,ad}$ species at 350 °C, it implies that these are active intermediates (Eq. (6)) and, therefore, their lifetime and population on the catalyst surface are too low to allow for their detection in the DRIFT spectra of Fig. 1B. The observation that adsorbed CO species are present on the catalyst surface under CO methanation reaction conditions indicates that the scission of the C–O bond may be the slow reaction step, in agreement with previous studies [45]. The weakening of the C–O bond strength in the presence of H_2 in the feed (Fig. 1B), indicates that its scission is favored in the presence of hydrogen and, therefore, results in an enhancement of the rate of the CO methanation reaction.

3.2.2. Methanation of CO_2

In Fig. 2A are shown DRIFT spectra obtained over the prereduced Ru/TiO_2 catalyst following exposure to 1%CO_2/He at 200 °C for 15 min (trace a) and subsequent addition of x%H_2 (x = 0–12) to the mixture (traces b–i). It is observed that interaction of CO_2 with the catalyst surface (trace a) does not give rise to bands in the ν(CO) region but results only in the development of bands located below 1700 cm^{-1}, which are due to formate/carbonate species associated with the support. The absence of bands attributable to Ru-bonded carbonyls indicates that dissociation of CO_2 does not take place under the present conditions, in agreement with results of previous studies [19,25,49]. However, addition of 0.45%H_2 in the feed results in the development of carbonyl bands located at 2066, 2012 and 1970(sh) cm^{-1} (trace b). Comparison with the spectrum obtained under a CO + H_2 mixture under otherwise the same conditions (Fig. 1A, trace b) shows significant differences in the nature and relative population of adsorbed CO species. In particular, the bands attributed to $Ru^{n+}(CO)_x$ species are either absent (band at 2136 cm^{-1}) or reduced significantly in intensity (band at 2066 cm^{-1}). This indicates that, under CO_2 + H_2 mixture, formation of partially oxidized sites produced by oxidative disruption of Ru crystallites and/or by dissociative adsorption of CO is significantly suppressed. Thus, the spectrum is dominated by bands at 2012 and 1970 cm^{-1}, attributable to Ru_x-CO and (TiO_2)Ru-CO species, respectively. These species may be formed via the RWGS reaction at the metal-support interface according to [16,17,19,20,22,23,25]:

$$CO_2 + H_{(Ru)} \rightarrow (COOH)_{(Ru-TiO_2)} \rightarrow CO_{(Ru)} + OH_{(TiO_2)} \quad (9)$$

Increase of H_2 concentration in the feed from 0.45% (trace b) to 12% (trace i) results in a decrease of the intensity of the 2066 cm^{-1} band and to a shift of the bands at 2012 and 1970 cm^{-1} toward lower wavenumbers (traces b–i). This is accompanied by the development of a weak band located at ca 3015 cm^{-1}, which is due evolution of CH_4 in the gas phase [15,25,29]. Conversion of CO_2 was also evidenced by measurements with the CO/CO_2 analyzer at the exit of the DRIFTS cell. It is of interest to note that interaction of the catalyst surface with CO_2 + H_2 mixture at 200 °C did not result in the development of bands attributable to $CH_{x,ad}$ species (Fig. 2A), in contrast to what was observed under CO + H_2 reaction conditions at the same temperature (Fig. 1A). This indicates that either the population of $CH_{x,ad}$ species is very small and/or that formation of surface carbon by dissociation of adsorbed carbonyls (Eq. (5)) is suppressed under CO_2 methanation conditions. The latter possibility is supported by the observation that the amount of oxidized Ru sites is decreased substantially under the present conditions. If this is the case, then methanation of carbonyl species produced by reaction (9) should not occur via the dissociative pathway represented by reaction (6). In fact, results of our recent study [25] provided evidence that methanation of CO_2 involves associative hydrogenation of adsorbed carbonyl species, as discussed below.

Similar DRIFT spectra obtained at 350 °C are presented in Fig. 2B. In agreement with results obtained at 200 °C, carbonyl bands in the ν(CO) region appear only after addition of hydrogen in the feed, verifying that the presence of H_2 is a prerequisite for the formation of adsorbed CO species on the catalyst surface. The spectrum recorded under flowing 1%CO_2 + 0.45% H_2 (in He) mixture is characterized by an asymmetric band at 2004 cm^{-1} (trace b), which shifts to 1980 cm^{-1} with increase of H_2 content to 12% (trace i). This is accompanied by evolution of CH_4 in the gas phase (band at 3015 cm^{-1}). Measurements with the CO/CO_2 analyzer at the exit of the DRIFT cell showed that significant amounts of CO were also produced in the gas phase, indicating that methanation of CO_2 occurs in parallel with the RWGS reaction. The conversion of CO_2 was more than 40% for H_2 contents higher than 5%.

It is of interest to note that the peak maximum in Fig. 2B appears at wavenumbers which are 20–40 cm^{-1} higher, compared to the corresponding ones obtained under CO + x%H_2 conditions (Fig. 1B). Following the same reasoning used above to discuss spectra of Fig. 1B, this may be interpreted by assuming that, under the CO_2 + x%H_2 reaction conditions of Fig. 2B, two carbonyl species are present on the catalyst surface, namely Ru_x-CO and (TiO_2)Ru-CO, both of which contribute to the band observed in the ν(CO) region. If this is the case, then the position of the combined band (which is located at relatively high wavenumbers) indicates that it consists mainly of Ru_x-CO species, i.e., that (TiO_2)Ru-CO species are more reactive and therefore their relative population is decreased.

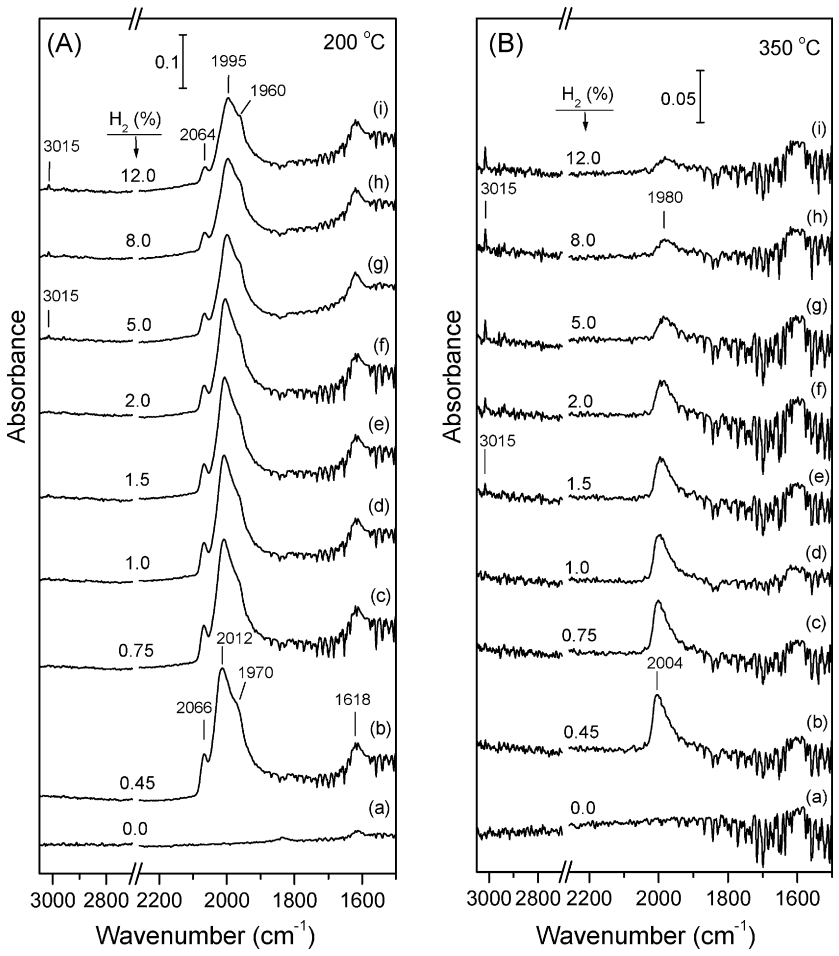

Fig. 2. DRIFT spectra obtained at (A) 200 °C and (B) 350 °C following interaction of Ru/TiO_2 catalyst with 1%CO_2 (in He) for 15 min (traces a) and subsequent exposure to 1%CO_2 + x%H_2 (x = 0.45–12%) mixtures (traces b–i).

Based on the above discussion, it may be argued that CO_2 methanation occurs via intermediate formation of adsorbed CO species produced via the RWGS reaction at the metal-support interface (Eq. (9)). Part of this species diffuses to the crystallite surface, as evidenced by detection of bands attributed to Ru_x-CO, and desorb to yield CO in the gas phase. The remaining (TiO_2)Ru-CO species, interact at the metal-support interface with adsorbed hydrogen atoms, to form a partially oxygenated carbonyl species and, eventually, methane in the gas phase. The relative rate of these pathways, which depends on feed composition and temperature, determines selectivity toward CH_4 (methanation) or CO (RWGS).

It should be noted that the associative pathway for methane formation may be also operable under CO methanation conditions, in addition to the dissociative pathway discussed above. This is in agreement with results of previous studies [11,50,51], which proposed that the mechanism of CO methanation reaction includes both dissociative and associative paths, the domination of the one or the other depending on the catalyst and experimental conditions employed. The dissociative path agrees well with the first reaction pathway described by Eq. (6), whereas the associative path involves interaction of adsorbed CO with adsorbed hydrogen, producing an oxygen-containing intermediate species which further hydrogenates toward CH_4:

$$CO_{(S)} + 2H_{(S)} \rightarrow (CHOH)_{(S)} + S \rightarrow (CH_x)_{(S)} + (OH_x)_{(S)} \rightarrow CH_4 + H_2O \quad (10)$$

Similar reaction schemes have been suggested by Sakakini [11] over Ru/Al_2O_3 catalysts and Sachtler et al. [51], who reported that the dissociative mechanism preferably occurs over Ni catalysts, whereas the formation of an intermediate oxygen-containing compound is enhanced over Ru catalysts. Although, no positive evidence for the existence of such intermediates was obtained in the present study, it is possible that a similar associative pathway is operable at higher temperature for the hydrogenation of Ru_x-CO species (Fig. 1B).

3.3. Effect of reaction temperature on CO/CO_2 methanation reactions studied by transient-MS technique

The interaction of the Ru/TiO_2 catalyst with reaction mixtures relevant to methanation of CO (0.5%CO + 5%H_2), CO_2 (1%CO_2 + 5%H_2) and CO/CO_2 (0.5%CO + 1%CO_2 + 5%H_2) (balance He) has been investigated employing the transient-MS technique at selected temperatures in the range of 200–500 °C, and results obtained are summarized in Figs. 3–5. For comparison purposes, in Fig. 6 are shown the equilibrium concentrations of CO, CO_2 and CH_4 as functions of reaction temperature for the above three feed compositions, calculated with the use of the Outokumpu HSC Chemistry® program.

3.3.1. Methanation of CO

The interaction of CO + H_2 reaction mixture with the Ru/TiO_2 catalyst was investigated at six selected temperatures in the range of 200–400 °C. For each experiment, the response curves of CO, CO_2,

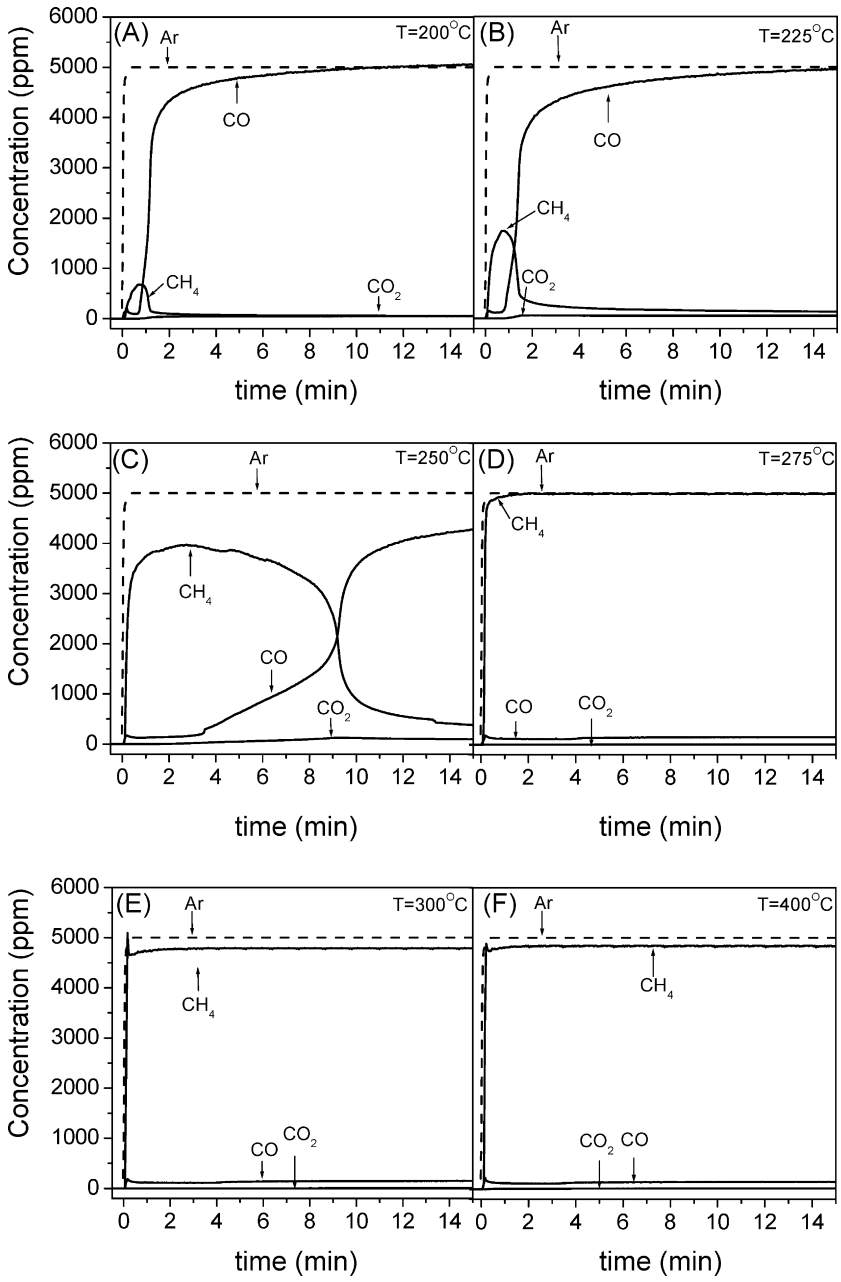

Fig. 3. Transient responses of gas phase CO, CO_2, CH_4 and Ar obtained from the prereduced Ru/TiO_2 catalyst following exposure to 0.5%CO + 5%H_2 + 0.5%Ar (in He) mixture at (A) 200, (B) 225, (C) 250, (D) 275, (E) 300 and (F) 400 °C.

H_2, CH_4 and Ar were recorded as functions of time-on-stream under the switch He→0.5%CO + 5%H_2 + 0.5%Ar (in He) over the prereduced catalyst sample. It is observed that, at 200 °C (Fig. 3A), the response of CH_4 appears immediately after the switch, while that of CO starts to increase with a delay of about 40 s, mainly due to adsorption on the catalyst surface. The concentration of CH_4 goes through a maximum after 45 s on stream and then abruptly drops close to zero, when CO starts to evolve at the effluent of the reactor. This indicates that although the reduced catalyst is initially active for CO methanation, its activity is practically lost after ca 1 min of exposure to the reaction mixture.

Qualitatively similar results were obtained at 225 °C (Fig. 3B), with the differences that (a) the concentration of CH_4 goes through a maximum that is about 3 times higher than that obtained at 200 °C, and (b) it does not drop to zero, at least for 30 min-on-stream. Increase of temperature to 250 °C (Fig. 3C) further improves the initial catalytic activity, as indicated by the substantial increase of the CH_4 concentration during the first minutes-on-stream. However, prolonged exposure to the reaction mixture results, again, in an abrupt decrease of the yield of CH_4 after ca 9 min, i.e., a time period which is much longer than that observed at lower temperatures. This behaviour indicates that processes that are responsible for the deactivation of the reduced catalyst when exposed to the reaction mixture become less important with increase of temperature. This becomes evident when the reaction temperature is increased to 275 °C (Fig. 3D), where conversion of CO to CH_4 reaches 100% and does not decrease for the time period this experiment lasted (30 min). Qualitatively similar results were obtained at 300 °C (Fig. 3E) and 400 °C (Figs. 3F), with the exception that small amounts of CO_2 were also produced in the gas phase, due to the onset of the WGS reaction (Fig. 6A).

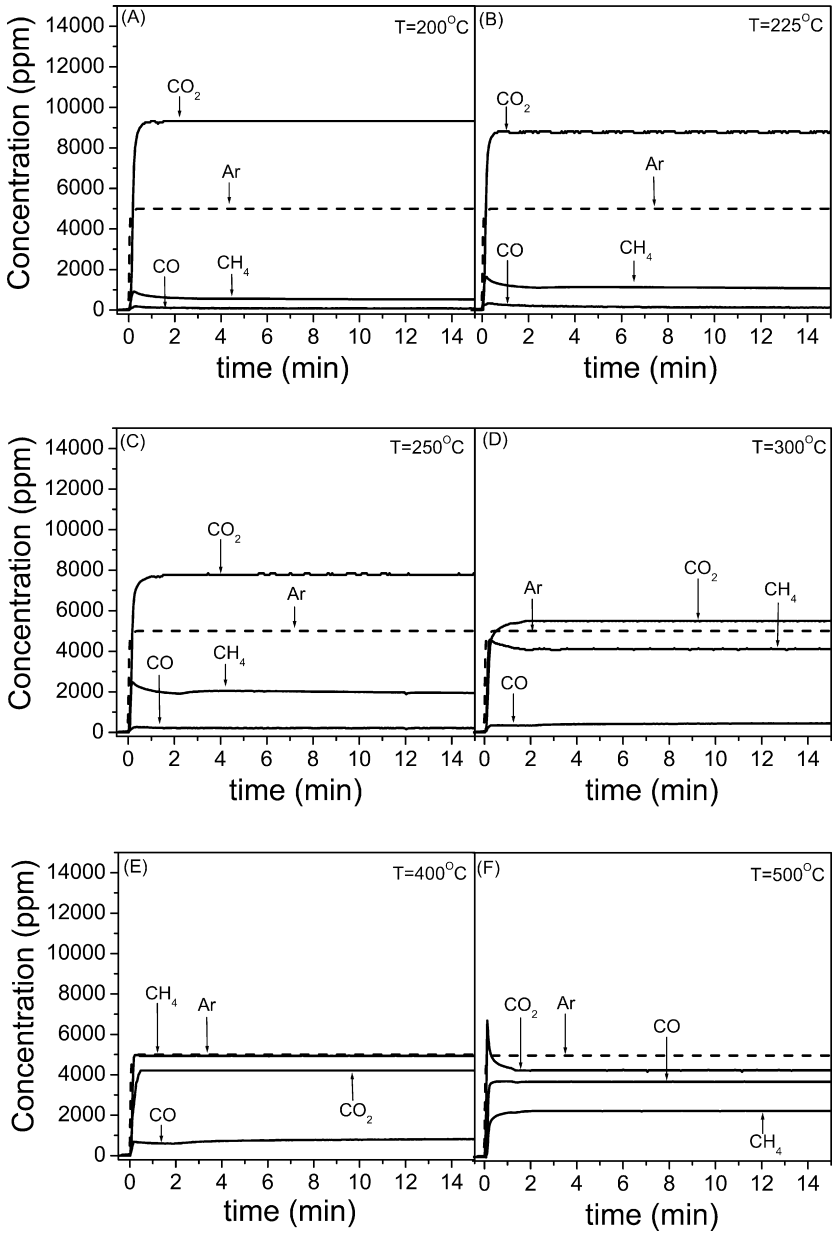

Fig. 4. Transient responses of gas phase CO, CO_2, CH_4 and Ar obtained from the prereduced Ru/TiO_2 catalyst following exposure to 1%CO_2 + 5%H_2 (in He) mixture at (A) 200, (B) 225, (C) 250, (D) 300, (E) 400 and (F) 500 °C.

Results of Fig. 3 may be understood by taking into account results of DRIFTS experiments presented in Fig. 1, and by considering the dissociative reaction mechanism that is operable under CO methanation conditions (Eq. (6)). The first step of this mechanism involves dissociation of adsorbed CO on reduced Ru crystallites and results in the formation of Ru–C and Ru–O species (Eq. (5)). The former react with adsorbed hydrogen atoms to yield methane (Eq. (6)), whereas the latter should be reduced by H_2 (Eq. (7)) in order to restore the catalytically active sites that are required for the dissociation of CO. As shown in Fig. 1A, the second condition is not fulfilled at temperature of 200 °C, where the catalyst surface is covered by a variety of carbonyls adsorbed on oxidized Ru sites. Thus, although the reduced catalyst is initially able to dissociatively adsorb CO and hydrogenate C into methane (Fig. 3A), its surface becomes eventually oxidized because the rate of reduction of Ru–O sites is much lower than that of CO dissociation and, therefore, production of CH_4 is suppressed or prevented. This seems to be the case for temperatures up to 250 °C (Fig. 3C). However, at temperatures higher than 275 °C reduction of Ru–O sites becomes fast enough so as to keep the catalyst surface in its reduced form and allow for the methanation reaction to proceed in a cyclic manner. This is supported by DRIFTS results of Fig. 1B, which do not show contributions from carbonyl species adsorbed on oxidized sites at temperature of 350 °C. In order to verify this assumption, a H_2-TPR was conducted over Ru/TiO_2 catalyst preoxidized at 300 °C in 20%O_2 flow for 30 min. Results obtained (not presented for brevity) showed that reduction of the so formed RuO_x species by hydrogen is initiated at temperatures around 250 °C.

3.3.2. *Methanation of CO_2*

The interaction of $CO_2 + H_2$ mixture with the pre-reduced Ru/TiO_2 catalyst was investigated with the transient-MS technique at six temperatures in the range of 200–500 °C, and results obtained after the switch, He → 1%CO_2 + 5%H_2 + 0.5%Ar (in He)

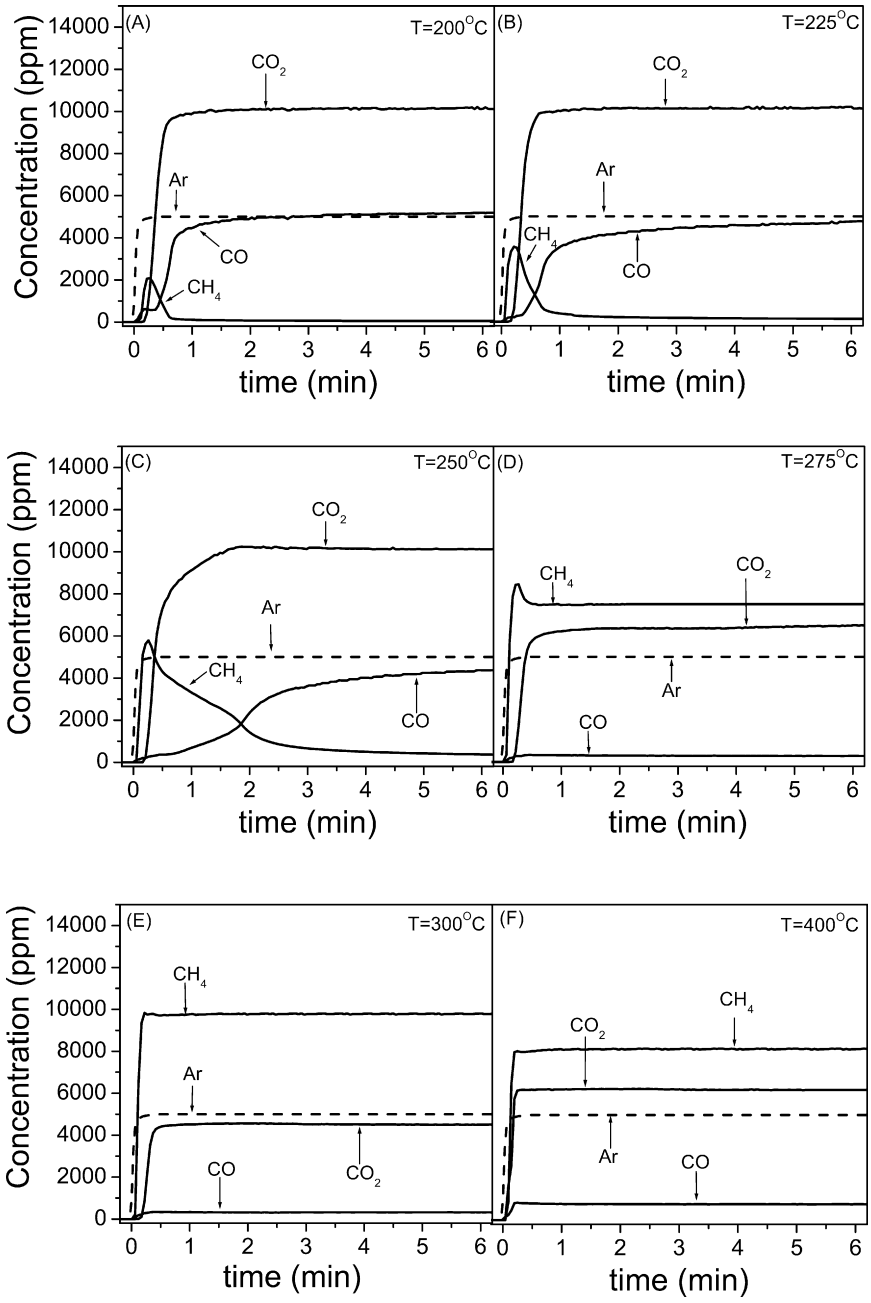

Fig. 5. Transient responses of gas phase CO, CO_2, CH_4 and Ar obtained from the prereduced Ru/TiO_2 catalyst following exposure to 0.5%CO + 1%CO_2 + 5%H_2 + 0.5%Ar (in He) mixture at (A) 200, (B) 225, (C) 250, (D) 275, (E) 300 and (F) 400 °C.

are presented in Fig. 4. It is observed that at 200 °C (Fig. 4A) the responses of CO_2 and CH_4 appear immediately after the switch and reach a steady state within less than 2 min-on-stream. Small amounts of CO are also detected, indicating that CO_2 hydrogenation occurs in parallel with the RWGS reaction at temperatures as low as 200 °C. Increase of reaction temperature from 200 to 500 °C (Fig. 4, A–F) results in a progressive increase of the conversion of CO_2, which goes through a maximum at 400 °C (Fig. 4E) and then decreases due to thermodynamic limitations [1,2,25] (Fig. 6B). At temperatures up to 400 °C, the yield of methane is significantly higher than that of CO, implying that methanation is strongly favored, compared to the RWGS reaction. The opposite is true at 500 °C, where CO production is significantly enhanced at the expense of CH_4, in agreement with previous studies over Ru/Al_2O_3 and Ru/TiO_2 catalysts [1,2,25].

Inspection of results presented in Fig. 4 shows that, in contrast to what was observed under CO + H_2 reaction conditions (Fig. 3), the activity of the catalyst does not decrease with time-on-stream even for temperatures as low as 200 °C. Based on the discussion made above, this implies that interaction of the reaction mixture with the catalyst surface does not result in oxidation of Ru crystallites, at least to an extent that would affect catalytic performance. This indicates that dissociation of CO_2 into Ru-CO and Ru–O species, which has been proposed to be the first step of CO_2 methanation [24,52], does not take place to an appreciable extent over the present reaction system. Thus, additional evidence is provided that carbonyls observed on the catalyst surface under reaction conditions (Fig. 2) are formed via the RWGS reaction at the metal-support interface (Eq. (9)). The small peak observed at 2066 cm^{-1} at 200 °C may be due to dissociation of Ru-CO, as discussed in the previous

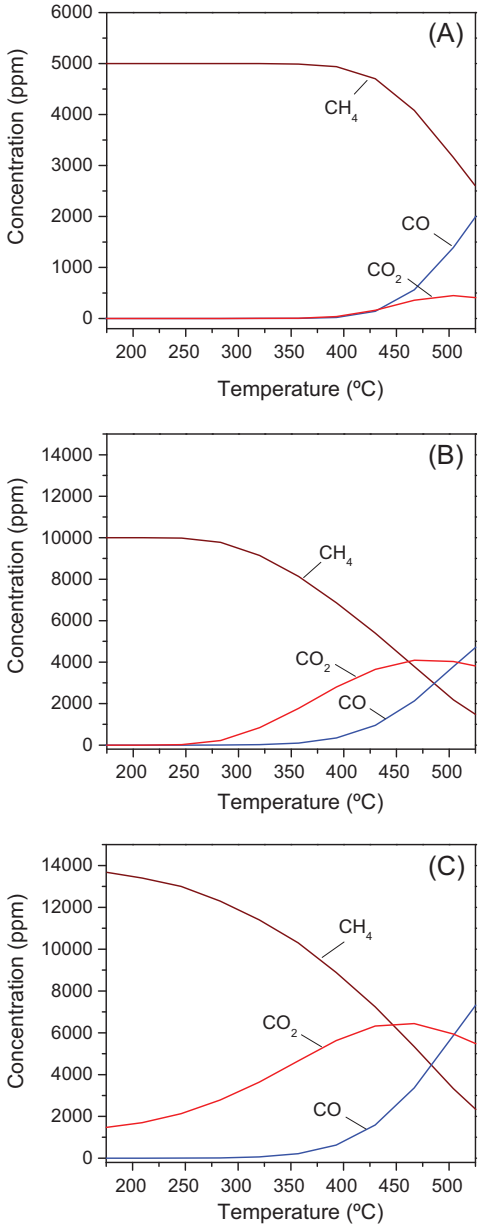

Fig. 6. Equilibrium concentrations of CO, CO_2 and CH_4 as functions of temperature calculated for feed compositions of (A) 0.5%CO + 5%H_2; (B) 1%CO_2 + 5%H_2; (C) 0.5%CO + 1%CO_2 + 5%H_2 (in He).

section. However, the dissociative route does not seem to be important under CO_2 methanation conditions over the present catalyst.

3.3.3. *Methanation of CO/CO_2 mixture*

The transient-MS responses obtained in the temperature range of 200–400 °C upon switching from He to the reaction mixture 0.5%CO + 1%CO_2 + 5%H_2 + 0.5%Ar (in He) are presented in Fig. 5. Results obtained at temperatures of 200–250 °C (Fig. 5, A–C) show that the responses of CH_4 and CO are qualitatively similar to those obtained in the absence of CO_2 in the same temperature range (Fig. 3, A–C). In particular, although the reduced catalyst is initially active for CO methanation, it loses its activity with time-on-stream after a certain period of time, which depends on reaction temperature. As discussed above, this can be attributed to accumulation of adsorbed oxygen species on the catalyst surface which cannot be removed efficiently in this temperature range. It is of great interest to note that, in spite of the fact that the catalyst was active for CO_2 methanation at 200–250 °C in the absence of CO in the feed (Fig. 4, A–C), the steady-state conversion of CO_2 is, practically, zero when both CO and CO_2 are present in the reaction mixture (Fig. 5, A–C). This indicates that the RWGS reaction at the metal-support interface (Eq. (9)), which is proposed to be the first step for CO_2 hydrogenation, is hindered in the presence of CO in the gas phase. This is the case both immediately after exposure to the reaction mixture, where the catalyst is in its reduced state, and after prolonged exposure to the reaction mixture, where ruthenium is partially oxidized. The delay observed between the response curves of CO_2 and Ar (~15 s at 200 °C), which is not accompanied by evolution of methane in the gas phase, indicates that an amount of CO_2 is adsorbed on the catalyst surface following interaction with the reaction mixture. A similar delay is observed when only CO_2 is present in the feed (Fig. 4), but cannot be easily discerned because of the different scale of the *x*-axis.

Increase of reaction temperature at 275 °C results in a completely different situation, in which the catalyst exhibits high activity and stability for the hydrogenation of both CO and CO_2 (Fig. 5D). In particular, conversions of CO and CO_2 reach values of 100% and 30%, respectively, which do not change for prolonged exposure to the reaction mixture (30 min in this experiment). This is accompanied by conversion of hydrogen, according to the stoichiometry of the two methanation reactions (Eqs. (1) and (2)). Conversion of reactants increases further at 300 °C (Fig. 5E) and then drops at 400 °C (Fig. 5F) due to thermodynamic limitations (Fig. 6C).

Results of Fig. 5 provide evidence that selective methanation of CO in CO/CO_2 mixtures takes place efficiently only under conditions where hydrogenation reactions occur predominantly via the dissociative route, compared to the associative route, because the latter also enhances the rates of CO_2 hydrogenation and RWGS reactions. When this condition is met, CO is selectively hydrogenated into methane. An open question still remains, related to the reason why hydrogenation of CO_2 is suppressed completely until conversion of CO reaches 100%. This issue will be the subject of our future investigations.

4. Conclusions

Mechanistic aspects of methanation of CO, CO_2 and CO/CO_2 mixtures have been investigated over 5%Ru/TiO_2 catalyst with the use of DRIFTS and transient mass spectrometry. Results obtained have been explained by considering that methanation of CO may take place via two reaction pathways: The first involves dissociative adsorption of CO on reduced Ru crystallites and subsequent hydrogenation of the so formed Ru–C and Ru–O species toward methane and water, respectively. At temperatures lower than ca 250 °C, adsorbed oxygen species cannot be removed efficiently and catalytic activity is suppressed due to progressive oxidation of catalytically active sites. Catalytic activity is restored at higher temperatures, due to reduction of partially oxidized sites by adsorbed hydrogen atoms. Under these conditions, the second route of CO methanation also becomes operable, which involves associative reaction of adsorbed CO species located at the metal-support interface. Methanation of CO_2 proceeds mainly through the second reaction pathway, with intermediate formation of adsorbed carbonyl species at the metal-support interface via the RWGS reaction. Selective methanation of CO in CO/CO_2 mixtures occurs efficiently under conditions where the dissociative reaction pathway is operable and the associative reaction pathway is completely suppressed.

References

[1] P. Panagiotopoulou, D.I. Kondarides, X.E. Verykios, Appl. Catal. B 88 (2009) 470–478.
[2] P. Panagiotopoulou, D.I. Kondarides, X.E. Verykios, Appl. Catal. A 344 (2008) 45–54.
[3] O. Görke, P. Pfeifer, K. Schubert, Catal. Today 110 (2005) 132–139.
[4] P. Panagiotopoulou, D.I. Kondarides, X.E. Verykios, Ind. Eng. Chem. Res. 50 (2011) 523–530.
[5] A.F. Ghenciu, Curr. Opin. Solid State Mater. Sci. 6 (2002) 389–399.
[6] T. Utaka, T. Takeguchi, R. Kikunchi, K. Eguchi, Appl. Catal. A 246 (2003) 117–124.
[7] R.A. Dagle, Y. Wang, G.G. Xia, J.J. Strohm, J. Holladay, D.R. Palo, Appl. Catal. A 326 (2007) 213–218.
[8] R.P. Underwood, C.O. Bennett, J. Catal. 86 (1984) 245–253.
[9] J.G. Ekerdt, A.T. Bell, J. Catal. 58 (1979) 170–187.
[10] N.W. Cant, A.T. Bell, J. Catal. 73 (1982) 257–271.
[11] B.H. Sakakini, J. Mol. Catal. A 127 (1997) 203–209.
[12] P. Biloen, J.N. Helle, W.M.H. Sachtler, J. Catal. 58 (1979) 95–107.
[13] N.M. Gupta, V.S. Kamble, R.M. Iyer, K. Ravindranathan Thampi, M. Grätzel, J. Catal. 137 (1992) 473–486.
[14] N.M. Gupta, V.P. Londhe, V.S. Kamble, J. Catal. 169 (1997) 423–437.
[15] S. Eckle, Y. Denkwitz, R.J. Behm, J. Catal. 269 (2010) 255–268.
[16] M. Marwood, R. Doepper, A. Renken, Appl. Catal. A 151 (1997) 223–246.
[17] M. Prairie, A. Renken, J.G. Highfield, K. Ravindranathan Thampi, M. Grätzel, J. Catal. 129 (1991) 130–144.
[18] M.V. Twigg, Catalyst Handbook, 2nd ed., Wolfe Publishing, London, 1989.
[19] F. Solymosi, A. Erdöhelyi, T. Bánsági, J. Catal. 68 (1981) 371–382.
[20] F. Solymosi, A. Erdöhelyi, M. Kocsis, J. Chem. Soc., Faraday Trans. 1 (77) (1981) 1003–1012.
[21] F. Solymosi, A. Erdöhelyi, M. Kocsis, J. Catal. 65 (1980) 428–436.
[22] N.M. Gupta, V.S. Kamble, V.B. Kartha, R.M. Iyer, K. Ravindranathan Thampi, M. Grätzel, J. Catal. 146 (1994) 173–184.
[23] C. Leitenburg, A. Trovarelli, J. Kašpar, J. Catal. 166 (1997) 98–107.
[24] M. Jacquemin, A. Beuls, P. Ruiz, Catal. Today 157 (2010) 462–466.
[25] P. Panagiotopoulou, D.I. Kondarides, X.E. Verykios, J. Phys. Chem. C 115 (2011) 1220–1230.
[26] P. Panagiotopoulou, D.I. Kondarides, J. Catal. 225 (2004) 327–336.
[27] P. Panagiotopoulou, A. Christodoulakis, D.I. Kondarides, S. Boghosian, J. Catal. 240 (2006) 114–125.
[28] P. Panagiotopoulou, D.I. Kondarides, J. Catal. 260 (2008) 141–149.
[29] C. Elmasides, D.I. Kondarides, S.G. Neophytides, X.E. Verykios, J. Catal. 198 (2001) 195–207.
[30] C. Elmasides, D.I. Kondarides, W. Grünert, X.E. Verykios, J. Phys. Chem. B 103 (1999) 5227–5239.
[31] H. Pfnür, D. Menzel, F. Hoffmann, A. Ortega, A.M. Bradshaw, Surf. Sci. 93 (1980) 431–452.
[32] C.S. Kellner, A.T. Bell, J. Catal. 71 (1981) 296–307.
[33] F. Solymosi, J. Raskó, J. Catal. 115 (1989) 107–119.
[34] L. Sabbatini, P.G. Zambonin, J. Electron. Spectrosc. Related Phenom. 81 (1996) 285–301.
[35] J.L. Robbins, J. Catal 115 (1989) 120–131.
[36] E. Guglielminotti, G.C. Bond, J. Chem. Soc. Faraday Trans. 86 (1990) 979–987.
[37] O.S. Alexeev, S.Y. Chin, M.H. Engelhard, L. Ortiz-Soto, M.D. Amiridis, J. Phys. Chem. B 109 (2005) 23430–23443.
[38] F. Boccuzzi, A. Chiorino, M. Manzoli, D. Andreeva, T. Tabakova, J. Catal. 188 (1999) 176–185.
[39] A. Yee, S.J. Morrison, H. Idriss, J. Catal. 191 (2000) 30–45.
[40] P. Panagiotopoulou, J. Papavasiliou, G. Avgouropoulos, T. Ioannides, D.I. Kondarides, Chem. Eng. J. 134 (2007) 16–22.
[41] A. Bensalem, J.C. Muller, D. Tessier, F. Bozon-Verduraz, J. Chem. Soc. Faraday Trans. 92 (1996) 3233–3237.
[42] P. Panagiotopoulou, D.I. Kondarides, Appl. Catal. B 101 (2011) 738–746.
[43] C.M. Kalamaras, P. Panagiotopoulou, D.I. Kondarides, A.M. Efstathiou, J. Catal. 264 (2009) 117–129.
[44] F. Solymosi, I. Tombacz, M. Kocsis, J. Catal. 75 (1982) 78–93.
[45] R.A. Dalla Betta, M. Shelef, J. Catal. 48 (1977) 111–119.
[46] H. Yamasaki, Y. Kobori, S. Naito, T. Onishi, K. Tamaru, J. Chem. Soc., Faraday Trans. 1 (77) (1981) 2913–2925.
[47] M.W. McQuire, C.H. Rochester, J. Catal. 141 (1993) 355–367.
[48] M. Primet, Catal. J. 88 (1984) 273.
[49] G.L. Haller, D.E. Resasco, Adv. Catal. 36 (1989) 173–235.
[50] C.K. Rofer-DePoorter, Chem. Rev. 81 (1981) 447–474.
[51] J.W.A. Sachtler, J.M. Kool, V. Ponec, J. Catal. 56 (1979) 284–286.
[52] G.D. Weatherbee, C.H. Bartholomew, J. Catal. 77 (1982) 460.